The Triad Targeting Signal of the Skeletal Muscle Calcium Channel Is Localized in the COOH Terminus of the α_{1S} Subunit

Bernhard E. Flucher, Nicole Kasielke, and Manfred Grabner

Department of Biochemical Pharmacology, University of Innsbruck, A-6020 Innsbruck, Austria

Abstract. The specific localization of L-type Ca^{2+} channels in skeletal muscle triads is critical for their normal function in excitation–contraction (EC) coupling. Reconstitution of dysgenic myotubes with the skeletal muscle Ca^{2+} channel α_{1S} subunit restores Ca^{2+} currents, EC coupling, and the normal localization of α_{1S} in the triads. In contrast, expression of the neuronal α_{1A} subunit gives rise to robust Ca^{2+} currents but not to triad localization. To identify regions in the primary structure of α_{1S} involved in the targeting of the Ca^{2+} channel into the triads, chimeras of α_{1S} and α_{1A} were constructed, expressed in dysgenic myotubes, and their subcellular distribution was analyzed with double immunofluorescence labeling of the α_{1S}/α_{1A} chimeras and the ryanodine receptor. Whereas chimeras containing the COOH terminus of α_{1A} were not incorporated into triads, chimeras containing the COOH terminus of α_{1S} were correctly targeted. Mapping of the COOH terminus revealed a triad-targeting signal contained in the 55 amino-acid sequence (1607–1661) proximal to the putative clipping site of α_{1S}. Transferring this triad targeting signal to α_{1A} was sufficient for targeting and clustering the neuronal isoform into skeletal muscle triads and caused a marked restoration of Ca^{2+}-dependent EC coupling.

Key words: calcium channel • dihydropyridine receptor • excitation–contraction coupling • immunofluorescence • skeletal muscle

Introduction

The precise localization of Ca^{2+} channels in specialized membrane domains is essential for their specific actions in multiple functions of excitable cells. In neurons, for example, voltage-gated Ca^{2+} channels located in the nerve terminal trigger neurotransmitter release and distinct populations of pre- and postsynaptic Ca^{2+} channels participate in different forms of synaptic plasticity (Berridge, 1998). In muscle cells, voltage-gated Ca^{2+} channels are specifically located in the intracellular junctions between the Ca^{2+} stores of the sarcoplasmic reticulum (SR)[1] and either the transverse tubules (t tubules) or the plasma membrane, called triads and peripheral couplings, respectively (Franzini-Armstrong and Jorgenson, 1994), in which the Ca^{2+} channel initiates excitation–contraction (EC) coupling (Melzer et al., 1995). Even though voltage-gated Ca^{2+} channels play such important roles in vital cell functions, the signals and mechanisms that direct and immobilize the different voltage-gated Ca^{2+} channel isoforms into their specific membrane domains are not known.

The skeletal muscle L-type Ca^{2+} channel (also called dihydropyridine receptor, DHPR) is composed of four subunits, the pore-forming α_{1S} and the accessory α_2/δ, β_{1a}, and γ_1 subunits (Catterall, 1996). The channel is concentrated in the junctional membranes of the triads (Jorgensen, 1989; Flucher et al., 1990), where it is in close contact with the Ca^{2+} release channels (ryanodine receptors, RyR) of the SR Ca^{2+} stores. Freeze-fracture analysis showed that in the triad junctions the DHPRs are arranged in square groups of four integral membrane particles called the tetrads and that their distribution pattern corresponds to that of the RyR arrays in the opposite SR membrane (Block et al., 1988). It is believed that the skeletal muscle DHPR functions as the voltage sensor for the gating of the SR Ca^{2+} release channel by a mechanism that is independent of Ca^{2+} influx through the L-type channel (Ríos et al., 1992). Thus, the highly orderly arrangement of DHPRs and RyRs in the triads is the structural basis for the depolarization-induced SR Ca^{2+} release in skeletal muscle EC coupling.

But what are the mechanisms by which the Ca^{2+} channels are specifically targeted into the triad junction and by which they achieve their characteristic organization? In skeletal muscle of the dysgenic mouse, which lacks the α_1

Address correspondence to Bernhard E. Flucher, Department of Physiology, University of Innsbruck, Fritz-Pregl-Str. 3, A-6020 Innsbruck, Austria. Tel.: 43-512-507-3787. Fax: 43-512-507-2836. E-mail: bernhard.e.flucher@uibk.ac.at

[1]*Abbreviations used in this paper:* DHPR, dihydropyridine receptor; EC, excitation–contraction; GFP, green fluorescent protein; nt, nucleotides; RE, restriction enzyme; RyR, ryanodine receptor; SR, sarcoplasmic reticulum; t tubule, transverse tubule.

subunit of skeletal muscle DHPR, triads form and RyRs are normally incorporated in these junctions in the absence of α_{1S} (Powell et al., 1996). Conversely, in myotubes of a skeletal RyR knock-out mouse, triads are also formed and DHPRs aggregate in these junctions, despite the absence of the RyR (Takekura et al., 1995); however, their arrangement in tetrads fails (Protasi et al., 1998). This suggests that triad targeting and tetrad formation are two independent processes and that interactions with the RyR are not necessary for the targeting of the DHPR into the junctional membrane domain of the triad. Evidence from studies in heterologous expression systems showing that coexpression of the DHPR α_1 subunit with β and α_2/δ increases membrane insertion of functional Ca^{2+} channels (Chien et al., 1995; Brice et al., 1997; Neuhuber et al., 1998a; Walker et al., 1998) suggests a role of the accessory Ca^{2+} channel subunits in the targeting process. Moreover, Ca^{2+} currents and EC coupling are deficient in skeletal myotubes of β-null mice and both functions can be reconstituted by heterologous expression of β_{1a} (Gregg et al., 1996; Beurg et al., 1997). Thus, expression of the β subunit is important for the efficient expression and functional insertion of the Ca^{2+} channel in the membrane, but not necessarily for its targeting into triads. Immunolocalization of α_2/δ and of recombinant β_{1a} expressed in dysgenic myotubes showed that, without the α_{1S} subunit, both subunits failed to be localized in the junctions (Flucher et al., 1991; Neuhuber et al., 1998b). Instead, the β and α_2/δ subunits required coexpression of α_{1S} for their own incorporation into the triads, suggesting that their own triad targeting is secondary to that of the α_{1S} subunit and that β and α_2/δ do not posses an independent targeting signal. The role of the γ subunit of the skeletal muscle Ca^{2+} channel is still poorly understood. However, the fact that EC coupling is not perturbed in skeletal muscle of a γ knock-out mouse also suggests that this subunit is not required for a function as important as the targeting of the Ca^{2+} channel complex into the triad (Freise et al., 2000). Thus, considering that the RyR and the accessory DHPR subunits either play no role in triad targeting of the DHPR or depend on the α_{1S} subunit for their own targeting into the junctions, the signal for triad targeting is likely to be contained within the α_{1S} subunit itself.

Here, we used heterologous expression of different α_1 subunit isoforms and isoform chimeras in dysgenic myotubes to identify the targeting signal in the skeletal muscle DHPR. Taking advantage of differential targeting properties of the skeletal muscle α_{1S} and the neuronal α_{1A} subunit, we generated a series of α_{1S}/α_{1A} chimeras and used them to localize the triad targeting signal in the COOH terminus of α_{1S}. The 55 amino acid sequence of α_{1S}, which is sufficient to confer triad targeting properties to α_{1A}, is the first description of a targeting signal of a voltage-gated Ca^{2+} channel to its native membrane domain.

Materials and Methods

Cell Culture and Transfections

Myotubes of the homozygous dysgenic (*mdg/mdg*) cell line GLT were cultured as described in Powell et al. (1996). At the onset of myoblast fusion (2–4 d after addition of differentiation medium), GLT cultures were transfected using DOTAP or FuGene (Boehringer). Cultures were analyzed 3–4 d after transfection.

Construction of Chimeric α_1 Subunits

The cDNA coding sequences of Ca^{2+} channel α_{1S}/α_{1A} subunit chimeras were inserted in-frame 3′ to the coding region of a green fluorescent protein (GFP), which was modified for thermal stability (Grabner et al., 1998) and contained in a proprietary mammalian expression vector (kindly provided by P. Seeburg, Zentrum für Molekulare Biologie, Heidelberg, Germany). Insertion of the cDNAs was accomplished as follows (nucleotide numbers, nt, are given in parentheses; asterisks indicate restriction sites introduced by PCR).

GFP-α$_{1S}$, GFP-α$_{1A}$. Construction of the GFP-tagged α_{1S} (Tanabe et al., 1987) and α_{1A} (Mori et al., 1991) subunits that were used as maternal clones for chimerization are described elsewhere (Grabner et al., 1998).

GFP-α$_1$SkNa. The α_{1A} (A) cDNA coding for the NH_2 terminus was fused to the α_{1S} (Sk) cDNA at position (nt A294/Sk154) using the "gene SOEing" technique (Horton et al., 1989). The SalI*-SacI fragment (nt 5′ polylinker-Sk651) of the cDNA product generated by the fusion PCR was coligated with the SacI–BglII fragment of Sk (nt 651–4488) into the corresponding SalI*/BglII restriction enzyme (RE) sites of plasmid GFP-α_{1S}.

GFP-α$_1$SkI-IIa. The HindIII–EcoRI fragment of Sk (nt 5′ polylinker-1007) and the EcoRI*-SphI A/Sk SOE fusion product (nt A1085–Sk1735) with the A/Sk transition at position (nt A1461/Sk1297) were coligated into the HindIII/SphI-cleaved polylinker of plasmid pSV-Sport1 (Life Technologies.). The SbfI–SphI fragment (nt 5′ polylinker-Sk1735) of this intermediate clone was coligated with the SphI–XhoI fragment of Sk (nt 1735–2654) into the corresponding SbfI/XhoI RE sites of plasmid GFP-α_{1S}.

GFP-α$_1$SkII-IIIm. The EcoRI–BalI fragment of Sk (nt 1007–1973) was coligated with the BalI–NdeI fragment (nt 1982–2296) from the muscle α_1 subunit (M) of *Musca domestica* (Grabner et al., 1994) into plasmid pSP72 (Promega) using the internal NdeI site (plasmid nt 2379) and the EcoRI site of the polylinker. The NdeI/EcoRI RE sites of pSP72 were also used to coligate two cDNA fragments, the NdeI*/XhoI fragment that was PCR generated from clone SkLC, a GFP-α_{1S} with a cardiac (C) II-III loop (nt C2716–Sk2654) (Grabner et al., 1999) plus the XhoI/BglII fragment of Sk (nt 2654–4488). The NdeI* primer was designed to introduce downstream of the NdeI* site additional *Musca* residues, A907G and S908T. In a subsequent step fragments EcoRI–NdeI (nt Sk1007–M2297) and NdeI*–BglII (C2716–Sk4488) were isolated from the pSP72 subclones and coligated into the EcoRI/BglII-cleaved pSP72 vector. Finally, the SalI–EcoRI fragment of Sk (nt 5′ polylinker-1007) was coligated with the EcoRI–BglII fragment (nt Sk1007–Sk4488) from the last pSP72 subclone into the SalI/BglII sites of plasmid GFP-α_{1S}.

GFP-α$_1$SkIII-IVa. The III-IV loop of the A cDNA was inserted into the corresponding Sk cDNA by a three-fragment SOE fusion PCR, thereby generating the transitions Sk/A (nt Sk3195/A4561) and A/Sk (nt A4725/Sk3355). The final PCR product was cleaved at its peripheral Sk XhoI/BglII RE sites and the resulting fragment (nt 2654–4488) was ligated into the corresponding XhoI/BglII sites of plasmid GFP-α_{1S}.

GFP-α$_1$Sa. The XhoI–SmaI fragment of Sk (nt 2654–4038) and the SmaI–BglII Sk/A cDNA fusion fragment (nt Sk4038–A5891) with the Sk/A transition (nt Sk4143/A5461) created by SOE PCR were coligated into the XhoI/BglII RE sites of plasmid GFP-α_{1A} (nt 1395/5891). Note that the XhoI sites are not corresponding RE sites and were used for subcloning only. Finally, the HindIII–XhoI fragment of Sk (nt 5′ polylinker-2654) was inserted into this HindIII/XhoI (nt 5′ polylinker/A1395, Sk2654) opened subclone to yield plasmid GFP-α_1Sa.

GFP-α$_1$As. The Xho–AccI fragment of A (nt 1395–4504) was coligated with the A/Sk SOE fusion fragment AccI–BglII (nt A4504–Sk4488) carrying its A/Sk transition at nt A5460/Sk4144, into the XhoI/BglII (nt 2654/4488) cleaved plasmid GFP-α_{1S}. Again, the A and Sk XhoI sites are not corresponding RE sites and were only used for subcloning. To yield GFP-α_1As, the SalI–EcoRI fragment from A (nt 5′ polylinker-1567) was coligated with the EcoRI–BglII fragment (nt A1567–Sk4488) after isolation from the subclone into the SalI/BglII (nt 5′ polylinker/4488) cleaved plasmid GFP-α_{1S}.

GFP-α$_1$Aas. The PCR generated BglII*–XbaI* fragment of Sk (nt 4566–4991) was inserted into the corresponding BglII/XbaI RE sites of plasmid GFP-α_{1A} (nt 5891/3′ polylinker). Upstream from the artificial XbaI* site of the Sk fragment, two stop codons (nt 4984–4989) were introduced to terminate the reading frame at residue T1661, which is close to the physiological clipping site of the α_{1S} carboxyl terminus (De Jongh et al., 1991).

GFP-α$_1$Aas(1524-1591). The BglII*–XbaI* Sk/A cDNA fusion fragment (nt Sk4566–A6347) with the Sk/A transition (nt Sk4773/A6118) generated by SOE PCR was ligated into the corresponding BglII/XbaI RE sites of plasmid GFP-α_{1A} (nt 5891/3′ polylinker). Again, two stop codons were introduced upstream of the artificial XbaI* site of the A portion of the fusion product (nt 6340–6345) to terminate the reading frame at residue G2113.

GFP-α$_1$Aas(1592-clip). The BglII–XbaI* A/Sk SOE fusion fragment (nt A5891–Sk4991) with the A/Sk transition at nt A6117/Sk4774 was ligated

into the corresponding BglII/XbaI RE sites of plasmid GFP-α_{1A} (nt 5891/3′ polylinker).

GFP-α_1A-clip. The BglII–XbaI* fragment of A (nt 5891–6347) was ligated into the corresponding BglII/XbaI RE sites of plasmid GFP-α_{1A} (nt 5891/3′ polylinker). Stop codons were introduced as in plasmid GFP-α_1Aas(1524–1591).

GFP-α_1Aas(1607-clip). The BglII–XbaI* A/Sk SOE fusion fragment (nt A5891–Sk4991) with the A/Sk transition at nt A6165/Sk4819 was ligated into the corresponding BglII/XbaI RE sites of plasmid GFP-α_{1A} (nt 5891/3′ polylinker).

All cDNA portions modified by PCR were checked for sequence integrity by sequence analysis (sequencing facility of MWG Biotech).

GFP and Immunofluorescence Labeling

Differentiated GLT cultures were fixed and immunostained as previously described (Flucher et al., 1994), using the monoclonal antibody 1A against the DHPR α_{1S} subunit at a final concentration of 1:1,000 (Morton and Froehner, 1987), the affinity purified antibody #162 against the type 1 RyR at a dilution of 1:5,000 (Giannini et al., 1995), and a monoclonal or an affinity purified anti–GFP antibody at a dilution of 1:2,000 and 1:4,000, respectively (Molecular Probes, Inc.). Alexa- and fluorescein-conjugated secondary antibodies were used with the anti–GFP antibodies so that the antibody label and the intrinsic GFP signal were both recorded in the green channel. Texas red–conjugated antibodies were used in double-labeling experiments to achieve a wide separation of the excitation and emission bands. Controls (for example, the omission of primary antibodies and incubation with inappropriate antibodies) were routinely performed. Images were recorded on an Axiophot microscope (Carl Zeiss, Inc.) using a cooled CCD camera and Meta View image processing software (Universal Imaging, Corp.).

Quantitative analysis of the labeling patterns was performed by systematically screening the coverslips for transfected myotubes using a 63× objective. The labeling pattern of positive myotubes with more than two nuclei were classified as either "clustered," "ER/SR," or "other" in the case that the labeled compartment was not clearly identifiable. The counts were obtained from several samples of at least three different experiments for each condition.

Patch-Clamp and Fluorescent Ca^{2+} Recording

Whole cell patch-clamp recordings were performed with an Axopatch 200A amplifier controlled by pClamp 8.0 software (Axon Instruments, Inc.). The bath solution contained (mM): 10 $CaCl_2$ or 3 $CaCl_2$ plus 7 $MgCl_2$, 145 tetraethylammonium chloride, and 10 HEPES (pH 7.4 with TEA-OH). Patch pipettes had resistances of 2–4 MΩ when filled with 145 Cs-aspartate, 2 $MgCl_2$, 10 HEPES, 0.1 Cs-EGTA, 2 Mg-ATP (pH 7.4 with Cs-OH). Leak currents were digitally subtracted by a P/4 prepulse protocol. Recordings were low-pass Bessel filtered at 2 kHz and sampled at 5 kHz. Currents were determined with 200-ms depolarizing steps from a holding potential of −80 mV to test potentials between −40 and +80 mV in 10-mV increments. Test pulses were preceded by a 1-s prepulse to −30 mV to inactivate endogenous T-type Ca^{2+} currents (Adams et al., 1990).

Action potential–induced Ca^{2+} transients were recorded in cultures incubated with 5 μM Fluo-4-AM plus 0.1% Pluronic F-127 (Molecular Probes, Inc.) in HEPES and bicarbonate-buffered DME for 45 min at room temperature, as previously described (Flucher et al., 1994; Powell et al., 1996). Action potentials were elicited by passing 1-ms pulses of 30 V across the 19-mm incubation chamber. 0.5 mM Cd^{2+} and 0.1 mM La^{3+} were added to block Ca^{2+} influx and therefore allow discrimination between Ca^{2+}-induced Ca^{2+} release and skeletal-type EC coupling. Application of 6 mM caffeine proved the functionality of SR Ca^{2+} release.

Results and Discussion

Reconstitution of Triad Targeting in Dysgenic Myotubes Transfected with the Skeletal Muscle Ca^{2+} Channel α_{1S} Subunit

Normal skeletal muscle in culture forms junctions between the SR and t tubules (triads and diads) and between the SR and the plasma membrane (peripheral couplings). These types of junctions are equivalent in function in that they support skeletal muscle type EC coupling, in molecular composition in that they contain RyRs in the SR and DHPRs in t tubules and plasma membrane, and in structure in that the two types of Ca^{2+} channels are organized in characteristic arrays of feet and tetrads, respectively. Therefore, we will henceforth use the terms "triad" and "triad targeting" in a generic sense to include all these types of junctions.

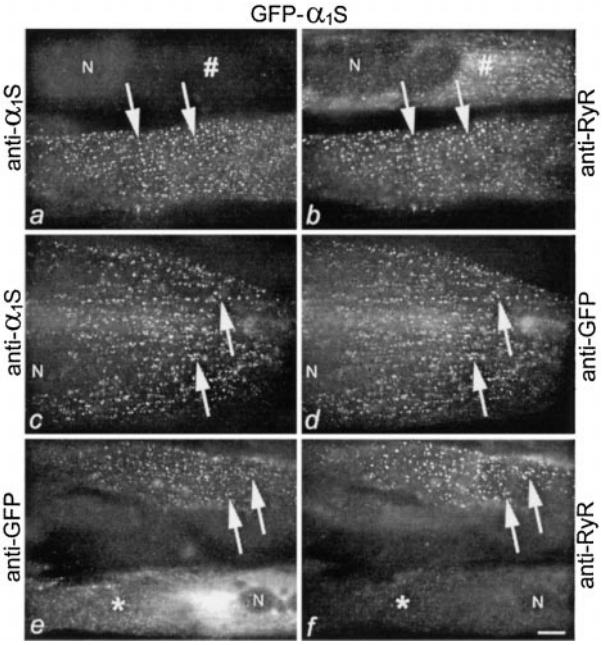

Figure 1. Normal incorporation of heterologously expressed GFP-α_{1S} in t tubule/SR junctions of dysgenic myotubes. (a and b) Double immunofluorescence labeling of α_{1S} subunits (a) and RyRs (b) shows that GFP-α_{1S} is colocalized with RyRs in clusters (examples indicated by arrows), presumably representing triad junctions and peripheral couplings. A nontransfected myotube in the same field (#) shows RyR clusters but no α_{1S} labeling. (c and d) Double staining of GFP-α_{1S} with antibodies against α_{1S} and against GFP shows that the fusion protein can be localized using either one of the antibodies. (e and f) As with anti–α_{1S} (a), clusters labeled with anti–GFP (e) are colocalized with RyR clusters (examples indicated by arrows). In poorly differentiated myotubes that lack RyR clusters (∗), GFP-α_{1S} accumulates in a reticular membrane system with densities in the perinuclear region, presumably the ER/SR network. N, nuclei. Bar, 10 μm.

Dysgenic muscle lacks the α_{1S} subunit of the L-type Ca^{2+} channel, but still forms regular junctions containing RyRs (Powell et al., 1996). Transient transfection of myotubes of the dysgenic cell line GLT with an expression plasmid encoding a fusion protein of the GFP and the α_{1S} subunit (GFP-α_{1S}) restores expression of the α_{1S} subunit in the triads, L-type Ca^{2+} currents, and skeletal muscle EC coupling (present study, and Grabner et al., 1998). Reconstitution of dysgenic myotubes with α_{1S} is well established and the properties observed here with the NH_2-terminal GFP-fusion protein are similar to those previously reported with a COOH-terminal GFP-fusion protein (Flucher et al., 2000) or to wild-type α_{1S} expressed in dysgenic myotubes (Tanabe et al., 1988).

The triad localization of GFP-α_{1S} can be detected in double immunofluorescence labeling experiments with antibodies against the α_{1S} subunit and against the RyR (Fig. 1, a and

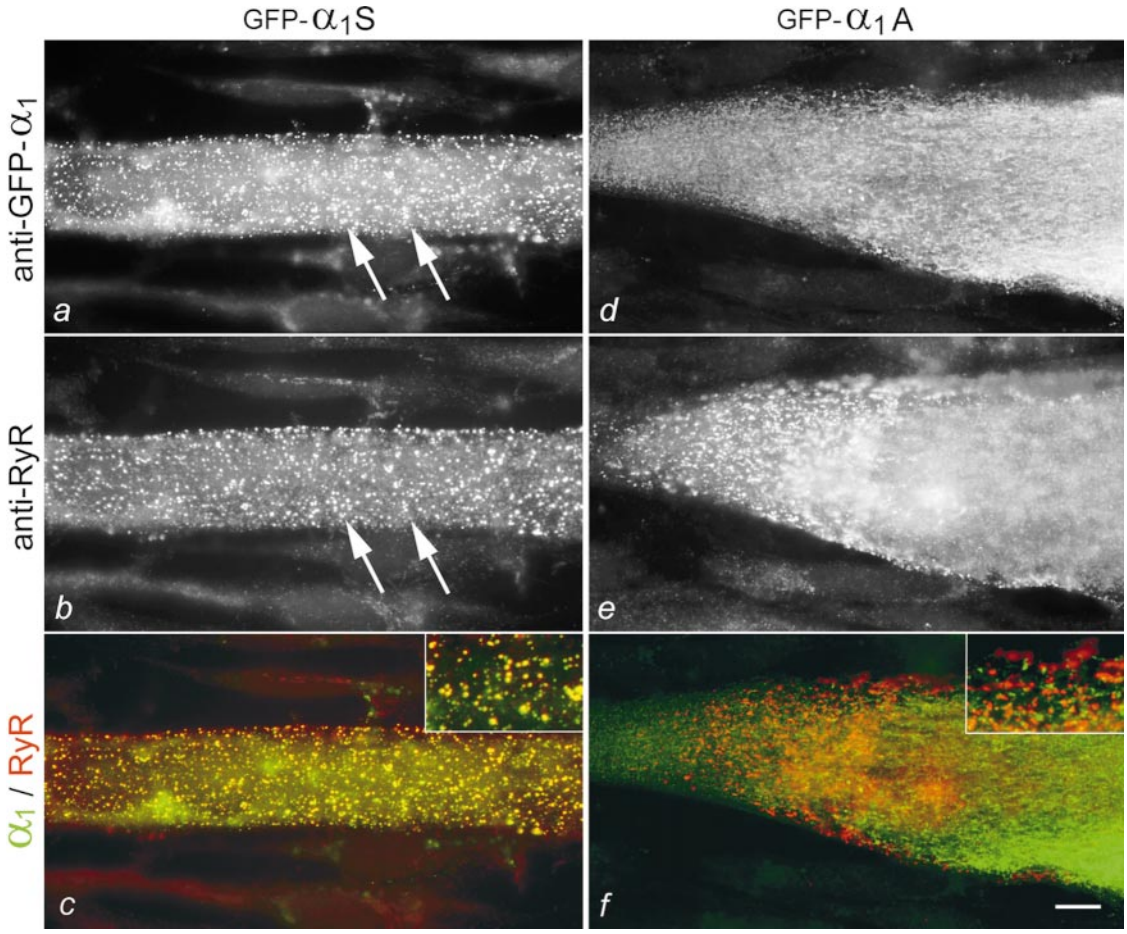

Figure 2. Differential targeting of GFP-α_{1S} and GFP-α_{1A} in transiently transfected dysgenic myotubes. Double immunofluorescence labeling of the skeletal GFP-α_{1S} and the neuronal GFP-α_{1A} (using anti–GFP for both) and of the RyR shows that only GFP-α_{1S} is colocalized with RyR clusters (a and b; examples indicated by arrows). GFP-α_{1A} is not colocalized with RyR clusters (d and e), but is retained in a reticular cytoplasmic membrane system, the ER/SR (d). (c and f) The differential subcellular distribution of GFP-α_{1S} and GFP-α_{1A} is highlighted in a color overlay of the images of a and b, and d and e, respectively (insets at twofold magnification). Colocalization of GFP-α_{1S} (green) with RyRs (red) results in yellow clusters. In contrast, separate green GFP-α_{1A} and red RyR labeling indicates the lack of colocalization of GFP-α_{1A} and RyRs. Bar, 10 μm.

b). Immunolabeling results in a punctate distribution pattern of anti–α_{1S} that is colocalized with similar clusters of anti–RyR. This clustered distribution pattern is characteristic of triad proteins in developing myotubes, and the coexistence of the t-tubule protein α_{1S} with the SR protein, the RyR, is indicative of their localization in junctions between the two membrane systems (Flucher et al., 1994). Myotubes not expressing GFP-α_{1S} form RyR clusters (Fig. 1 b), which have previously been shown to correspond to t tubule/SR junctions by electron microscopy (Powell et al., 1996).

Double immunofluorescence labeling of GFP-α_{1S} with anti–GFP and anti–α_{1S} (Fig. 1, c and d) or with anti–GFP and anti–RyR (e and f) results in the same clustered distribution pattern in equally large fractions of GFP-α_{1S}–expressing myotubes (57 and 58%, respectively). Therefore, we continued using anti–GFP for the immunolocalization of GFP-α_1 constructs, because it recognizes both GFP-α_{1S} and GFP-α_{1A}, allowing the direct comparison of the labeling patterns of all chimeras used in this study. Fig. 1 e also shows a myotube in which the GFP-α_{1S} is expressed but its labeling pattern is not clustered. Instead it is distributed throughout a tubular membrane system that is very dense in the perinuclear region and has previously been identified as the ER/SR (Powell et al., 1996; Flucher et al., 2000). ER/SR distribution of heterologously expressed α_1 subunits can be observed with all constructs and occurs preferentially in poorly differentiated cells; i.e., myotubes in which triads are not formed. The myotube shown in Fig. 1, e and f, for example, lacks RyR clusters, indicating that triad junctions, and thus the target for GFP-α_{1S}, was missing and therefore GFP-α_{1S} was retained in the biosynthetic apparatus. However, in addition to myotubes lacking the target for the α_1 subunit, retention in the ER/SR system can also be observed in normally differentiated myotubes if they are transfected with α_1 constructs lacking the triad targeting signal (see below).

Differential Targeting of the Skeletal and the Neuronal Ca^{2+} Channel α_1 Subunits Expressed in Dysgenic Myotubes

Fig. 2 shows a direct comparison of the labeling patterns of the skeletal muscle GFP-α_{1S} and the neuronal GFP-α_{1A} expressed in dysgenic myotubes. Whereas double immunolabeling with anti–GFP and anti–RyR reveals the colocalization of GFP-α_{1S} and RyR in the junctions (Fig. 2, a–c), GFP-α_{1A} is localized exclusively in the ER/SR network (d),

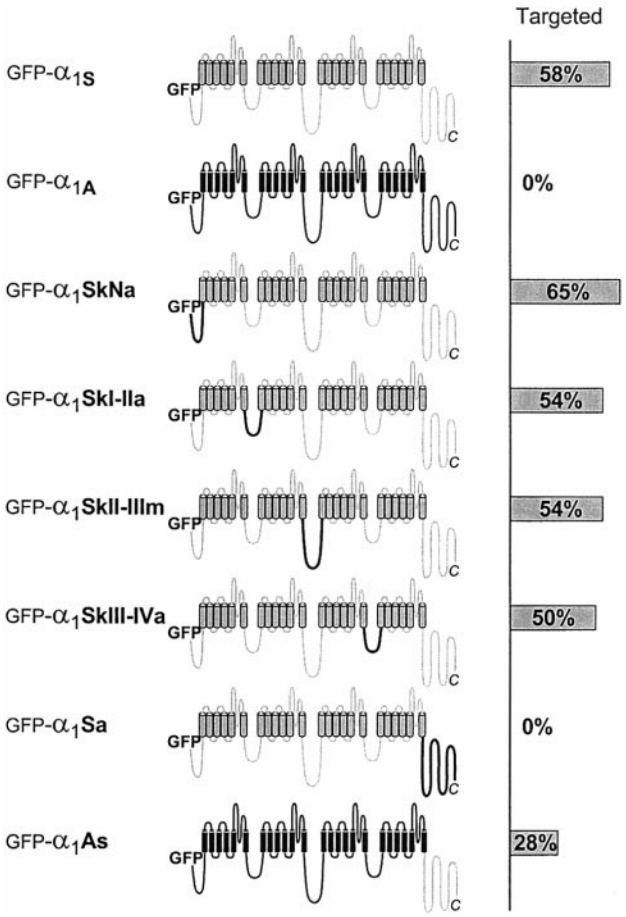

Figure 3. Screening for the molecular location of the triad targeting signal in α_{1S}/α_{1A} chimeras. Schematic representation of the membrane topology of the α_1 subunit isoforms and chimeras with α_{1S} sequences in gray and α_{1A} sequences in black. Large cytoplasmic portions of α_{1S} were systematically replaced by the corresponding sequences of α_{1A} (or in the case of GFP-α_1SkII-IIIm of the *Musca* α_1 sequence). The bar graph at the right shows the percentage of transfected myotubes in which the expressed α_1 subunit isoform/chimera achieved a clustered distribution indicative of correct triad targeting.

even though the presence of RyR clusters (e) indicates the normal differentiation of junctions. The merged color images of GFP-α_1 in green and RyR in red further emphasizes the differential targeting of the skeletal and neuronal channels. Here, colocalization of GFP-α_{1S} with RyR shows up as yellow clusters (c), whereas the distinct localization of GFP-α_{1A} in the ER/SR and RyR in clusters is seen as separate green and red label, respectively (f). Quantification of the labeling patterns in at least six independent experiments showed that, while the overall expression of both constructs was the same, clusters were observed in 58% (n = 967) of the myotubes transfected with GFP-α_{1S}, but never in myotubes expressing GFP-α_{1A} (n = 418). Thus, GFP-α_{1A} fails to be incorporated into triad junctions.

To exclude the possibility that the absence of GFP-α_{1A} resulted from improper folding or lack of plasma membrane incorporation of the GFP-α_{1A} construct rather than lack of a triad targeting signal, we performed patch-clamp recordings of myotubes expressing this construct. Even though a plasma membrane stain was not detected with immunocytochemistry in GFP-α_{1A}–transfected myotubes, the whole-cell recordings showed large Ca^{2+} currents with the macroscopic properties of class-A Ca^{2+} channels expressed in heterologous mammalian expression systems (example shown in Fig. 6, below) (Adams et al., 1994). Thus, GFP-α_{1A} expressed in dysgenic myotubes formed functional channels in the cell membrane. But instead of becoming locally concentrated in the triads, GFP-α_{1A} was distributed diffusely in the plasma membrane at densities below detectability with immunocytochemistry.

Recordings of cytoplasmic Ca^{2+} transients in response to electrical field stimulation showed that GFP-α_{1S} regularly restored skeletal muscle EC coupling in dysgenic myotubes (see Fig. 7, and Powell et al., 1996; Flucher et al., 2000). In contrast, restoration of EC coupling by GFP-α_{1A} was only rarely observed (see below). Thus, both the skeletal muscle GFP-α_{1S} isoform and the neuronal GFP-α_{1A} isoform were functionally expressed in dysgenic myotubes, but only GFP-α_{1S} was targeted into the triad junctions and efficiently restored EC coupling. The differential distribution of GFP-α_{1S} and GFP-α_{1A} as well as their functional differences are in general agreement with observations from a previous study comparing the expression of GFP-α_{1S}, GFP-α_{1A}, and a cardiac GFP-α_{1C} construct in primary cultured dysgenic myotubes (Grabner et al., 1998). In that study, GFP-α_{1A} differed from the muscle isoforms in that its distribution patterns were restricted to near the injection site and that only GFP-α_{1A} failed to respond in a contraction assay. Together, these data support our hypothesis that the skeletal muscle α_{1S} contains a signal for its targeting and selective incorporation into triads, but that such a triad targeting signal is missing from the neuronal α_{1A} subunit isoform.

Localization of the Triad Targeting Site to the COOH Terminus of the α_{1S} Subunit

With a properly targeted GFP-α_{1S} and a nontargeted GFP-α_{1A} in our hands, we decided to start screening for the location of the targeting signal by replacing the prominent cytoplasmic portions of GFP-α_{1S} with the corresponding sequences of α_{1A}. GFP-α_{1S}/α_{1A} chimeras were generated with the following portions of α_{1A} (Fig. 3): the NH_2 terminus (GFP-α_1SkNa), the cytoplasmic loop connecting repeats I and II (GFP-α_1SkI-IIa) or that connecting repeats III and IV (GFP-α_1SkIII-IVa), and the COOH terminus (GFP-α_1Sa). Because the II-III loop of α_{1A} is more than three times the size of that of α_{1S}, we were concerned that it might impede appropriate incorporation of a chimera, not because of lacking a triad targeting signal, but because of sterical hindrance. Instead, the II-III loop of the house fly (*M. domestica*) α_1 subunit (Grabner et al., 1994) was used for constructing a II-III chimera (GFP-α_1SkII-IIIm). Its II-III loop has similar size as that of the rabbit skeletal muscle α_{1S} but shows very little sequence homology to α_{1S} and, like α_{1A}, the *Musca* α_1 subunit failed to be targeted into the junctions. Double immunolabeling with anti–GFP and anti–RyR and subsequent analysis of the targeting properties revealed that all of these chimeras with the exception of GFP-α_1Sa were clustered together with the RyR. The clustering efficiencies were between 50 and 65% (n = 200) for each construct, which was similar to that of GFP-α_{1S} (Fig. 3). Thus, neither the NH_2 terminus nor any of the major cytoplasmic loops of α_{1S} are essential for triad targeting.

The I-II loop contains the interaction domain for the β subunit (Pragnell et al., 1994). Association of the β subunit

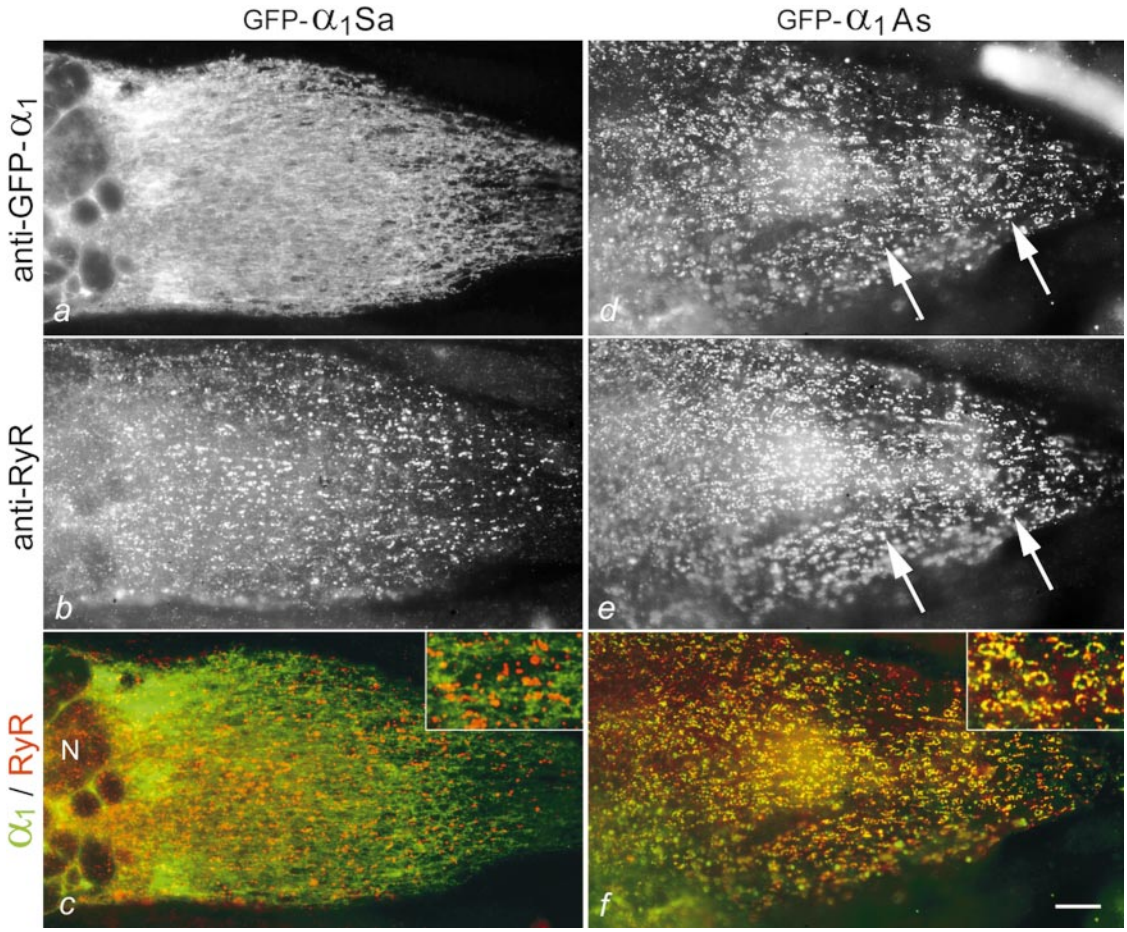

Figure 4. Exchange of the targeting properties between GFP-α_{1S} and GFP-α_{1A} by swapping their COOH-terminal tails. (a and b) Expression of an α_{1S} chimera with the COOH terminus of α_{1A} (GFP-α_1Sa) in dysgenic myotubes results in a loss of triad targeting; instead, GFP-α_1Sa was consistently localized in the ER/SR system. (d and e) The converse chimera, GFP-α_1As, has gained the ability to become coclustered with RyRs in the junctions (examples indicated by arrows). (c and f) The color overlays show the lack of colocalization of GFP-α_1Sa and RyR clusters, but a high degree of colocalization of clustered GFP-α_1As and RyRs (insets at twofold magnification). Red and green clusters in f are mostly due to differences in labeling intensities and not due to differential distribution of GFP-α_1As and RyR (compare d and e). N, nuclei. Bar, 10 μm.

with this loop has been implicated in an important early step in membrane insertion of Ca^{2+} channels (Bichet et al., 2000). The I-II loop at least of α_{1A} seems to contain an ER retention signal that is blocked upon association with β to release the complex from the ER. Since the β interaction domain in the I-II loop is shared by all known α_1 subunits and a β subunit is endogenously expressed in dysgenic myotubes, a negative effect on triad targeting due to this mechanism was not to be expected with the GFP-α_1SkI-IIa chimera. The II-III loop of α_{1S} contains the sequence important for the interaction with the RyR. It specifies the tissue-specific mode of EC coupling (Tanabe et al., 1990a) and the amplification of Ca^{2+} currents by association with the skeletal type 1 RyR (Nakai et al., 1996; Grabner et al., 1999). Therefore, it is quite remarkable that replacement of the α_{1S} II-III loop by a loop as different as that of *Musca*'s α_1 subunit had no adverse effect on triad targeting of chimera GFP-α_1SkII-IIIm. On the other hand, the finding that the molecular domain responsible for DHPR-RyR interactions is not essential for triad targeting is consistent with the observations showing that, in the RyR1 knock-out mouse, α_{1S} clusters in the junctions despite the lack of RyR1 (Takekura et al., 1995).

Replacing the COOH terminus of GFP-α_{1S} with that of α_{1A} (GFP-α_1Sa) disrupted triad targeting (Fig. 4, a–c). Similar to the distribution pattern described above for GFP-α_{1A}, GFP-α_1Sa was found in the ER/SR system, but never in clusters together with the RyR. Ca^{2+} currents in GFP-α_1Sa-transfected cells were very small and frequently below detectability. This is not surprising for skeletal Ca^{2+} channels not localized in the triad junctions. Nakai et al. (1996) and Grabner et al. (1999) have shown that skeletal muscle α_{1S} requires the specific interaction with type 1 RyR in the junctions for the expression of normal current densities. Both the absence of RyR1 in dyspedic myotubes and the interruption of the interaction between α_{1S} and the RyR resulted in a considerable attenuation of skeletal Ca^{2+} currents. Similarly, it is to be expected that in addition to decreased membrane insertion, the failure of triad targeting of GFP-α_1Sa and the associated lack of interactions with the RyR would result in the attenuation of Ca^{2+} currents.

The failure of triad targeting in the GFP-α_1Sa chimera suggests that the triad targeting signal may be contained within the COOH terminus of α_{1S}. To verify this interpretation, the corresponding reverse chimera, GFP-α_{1A} with the COOH terminus of α_{1S} (GFP-α_1As) was constructed.

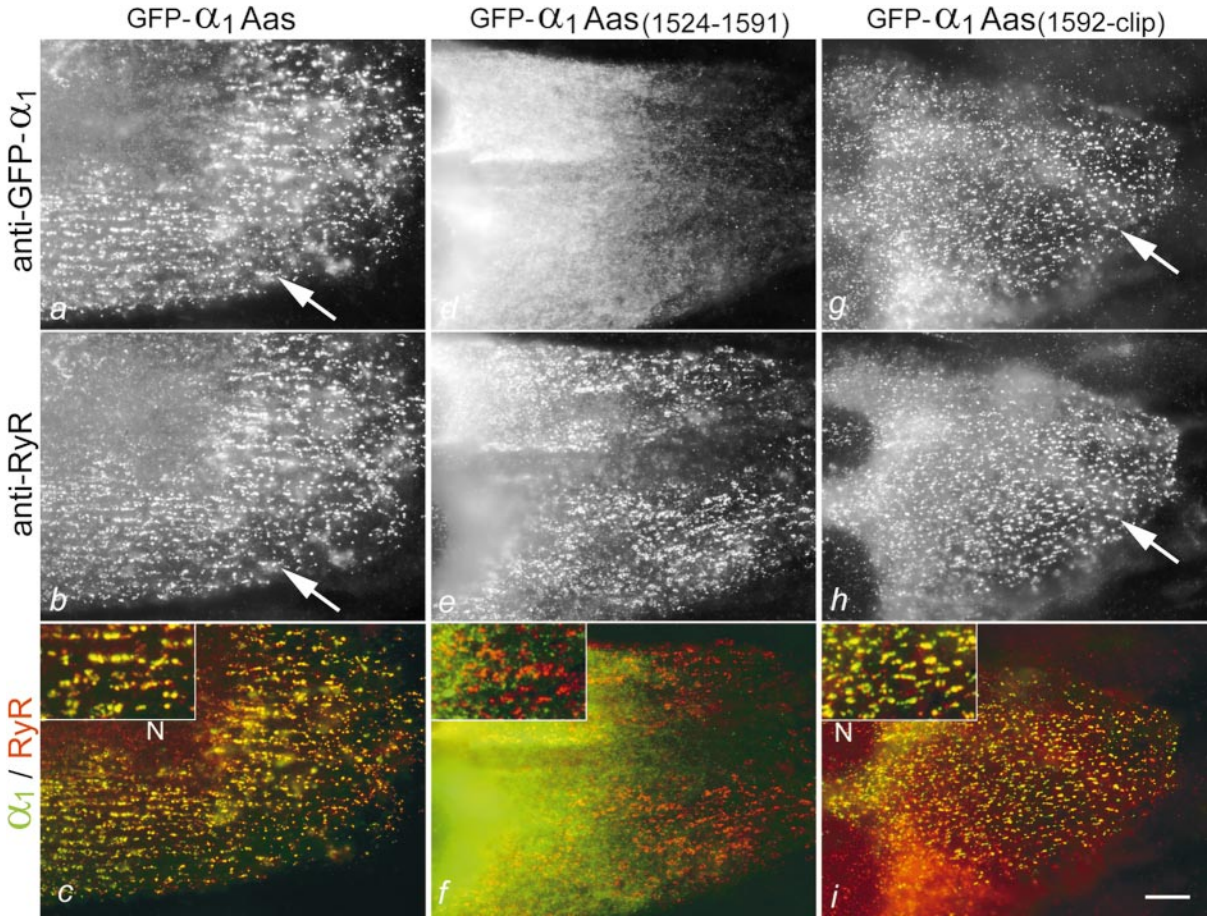

Figure 5. Localization of the triad targeting signal within the COOH-terminal tail of α_{1S}. (a–c) Chimera GFP-α_1Aas consisting of the body plus the first 145 COOH-terminal residues of α_{1A} and the remaining COOH terminus of α_{1S} ending at the putative clipping site at position 1661 is readily targeted into the junctions when expressed in dysgenic myotubes (example indicated by arrows). (d–f) Chimera GFP-α_1Aas$_{(1524\text{-}1591)}$ containing only the proximal half of this COOH-terminal α_{1S} sequence fails to be targeted into the junctions. (g–i) However, chimera GFP-α_1Aas$_{(1592\text{-clip})}$ containing the distal half of this COOH-terminal α_{1S} sequence is efficiently targeted into junctions of t tubules and plasma membrane with the SR (example indicated by arrows). (c, f, and i) Color overlays of images shown above; insets at twofold magnification. N, nuclei. Bar, 10 μm.

When expressed in dysgenic myotubes, GFP-α_1As was found coclustered with the RyR (Fig. 4, d–f). The efficiency of clustering was somewhat reduced compared with wild-type GFP-α_{1S} (28% of 1,479 transfected myotubes from eight separate experiments; Fig. 3); however, it was clear that by replacing its COOH terminus with that of α_{1S}, this otherwise class-A channel gained the ability to be targeted into the triad junctions. Ca^{2+} currents with properties similar to those of GFP-α_{1A} were expressed (see Fig. 6 b), indicating that this channel chimera was functional. Since swapping the COOH termini of α_{1S} and α_{1A} conferred triad targeting properties to the neuronal isoform (GFP-α_1As) and disrupted triad targeting in the skeletal muscle Ca^{2+} channel isoform (GFP-α_1Sa), it was evident that the signal responsible for this specific localization must be contained in the COOH terminus of α_{1S}.

Localization of the Triad Targeting Signal within the COOH Terminus of α_{1S}

The skeletal muscle α_{1S} subunit isolated from muscle preparations exists in two size forms, the minor fraction corresponding to the full-length α_{1S} sequence and the major fraction corresponding to a COOH-terminally truncated α_{1S}, lacking the sequences distal to approximately residue 1661 (De Jongh et al., 1991). Although truncation occurs after incorporation of α_{1S} into the junctions (Flucher et al., 2000), the truncated form by itself is sufficient to restore skeletal muscle EC coupling in dysgenic myotubes (Beam et al., 1992), suggesting that it is correctly inserted into the junctions. Therefore, it seemed unlikely that the triad targeting signal resides in the part of the COOH terminus distal to the putative clipping site. Sequence comparison of different α_1 subunit isoforms showed that the first 140 residues of the COOH terminus are highly homologous, followed by a stretch of similar length with much lower sequence homology. Thus, we concentrated our search for the triad targeting signal on the stretch in between the highly homologous region and the putative clipping site of α_{1S}. We created one chimera (GFP-α_1Aas) with the skeletal sequence 1524–1661 substituted for the corresponding region of α_{1A}, and two daughter chimeras, each containing one half of that region from α_{1S} (see Fig. 6 a). GFP-α_1Aas$_{(1524\text{-}1591)}$, which contains the proximal half of this region from α_{1S} (1524–1591) and the distal half from α_{1A}, ends at an arbitrary site of α_{1A} corresponding to the location of the clipping site in α_{1S}, because α_{1A} does not con-

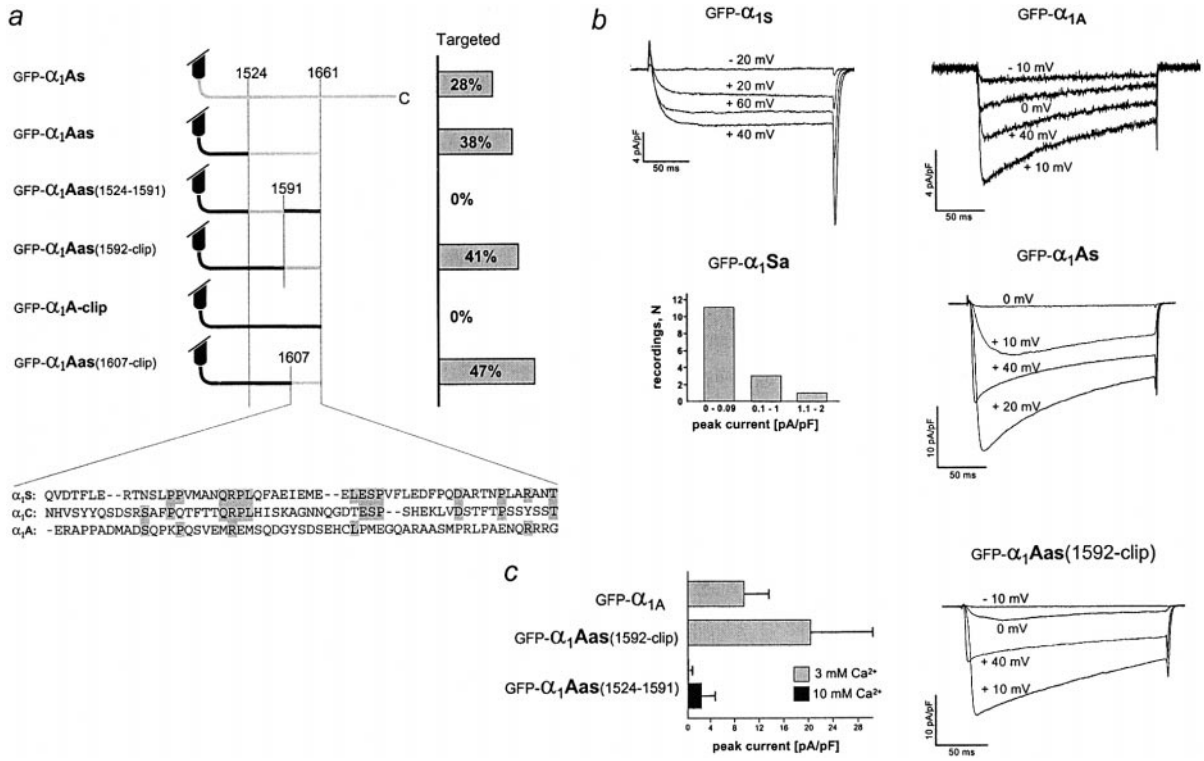

Figure 6. Targeting properties and current properties of wild-type α_1 subunit isoforms and COOH-terminal chimeras. (a) Isoform sequence composition of COOH termini in the studied chimeras, with sequences of α_{1S} in gray and α_{1A} in black. Bar graph indicates the percentages of transfected myotubes showing triad targeting in immunofluorescence analysis. Alignment of the 55 α_{1S} amino acids containing the targeting signal with the corresponding sequences of α_{1C} and α_{1A}. (b) Representative current traces recorded from dysgenic myotubes transfected with wild-type GFP-α_{1S} (in 10 mM Ca^{2+}), with GFP-α_{1A} or with the targeted chimera GFP-α_1As (both in 3 mM Ca^{2+}). Currents from GFP-α_1Sa (in 10 mM Ca^{2+}) were too small for systematic analysis; see frequency distribution of current densities. (c) Representative current trace of the targeted chimera GFP-α_1Aas$_{(1592\text{-clip})}$ and comparison of peak current densities recorded from GFP-α_{1A}, GFP-α_1Aas$_{(1592\text{-clip})}$, and GFP-α_1Aas$_{(1524\text{-}1591)}$. Substituting COOH-terminal α_{1A} sequence with the skeletal sequence 1592–1661 results in a twofold increase of current density compared with GFP-α_{1A}, whereas substituting for skeletal sequence 1524–1591 reduces the current densities to near the detection level and could be analyzed only after increasing the Ca^{2+} concentration to 10 mM (n = 7–17).

tain this putative clipping site itself. GFP-α_1Aas$_{(1592\text{-clip})}$ is neuronal up to residue 2039 of α_{1A}, with the distal part of α_{1S}, from residue 1592 to the putative clipping site (1661).

Fig. 5, a–c, shows that GFP-α_1Aas was correctly targeted into the triad junctions. 38% (n = 1,602) of the transfected myotubes showed a clustered distribution of GFP-α_1Aas colocalized with RyR immunolabel. This confirmed that the region beyond residue 1661, which can be subject to truncation, is not necessary for triad targeting. Rather, the triad targeting signal is contained in the sequence between residues 1524 and 1661 of α_{1S}. Within this region, the proximal half did not confer triad targeting properties to α_{1A}. Not a single myotube out of 887 GFP-α_1Aas$_{(1524\text{-}1591)}$–transfected myotubes showed a clustered distribution pattern of this α_1 chimera; instead, GFP-α_1Aas$_{(1524\text{-}1591)}$ was regularly found in the ER/SR (Fig. 5, d–f). In contrast, its sister chimera GFP-α_1Aas$_{(1592\text{-clip})}$ was efficiently targeted to the junctions (Fig. 5, g–i). 41% (n = 1,076) of the transfected myotubes showed a clustered distribution of GFP-α_1Aas$_{(1592\text{-clip})}$ colocalized with the RyR, indicating that this 70 amino acid sequence contains the triad targeting signal. To further restrict the region containing the triad targeting signal, one more chimera was created with only the last 55 residues proximal to the putative clipping site from α_{1S} (GFP-α_1Aas$_{(1607\text{-clip})}$). This construct was also found in clusters in 47% (n = 603) of the transfected myotubes (Fig. 6 a; immunofluorescence image not shown), demonstrating that the 55 amino acid segment between residues 1607

Table I. Restoration of Action Potential-induced Ca^{2+} Transients in Dysgenic Myotubes Expressing Different α_1 Subunit Isoforms and the Targeted Chimera GFP-α_1Aas$_{(1592\text{-clip})}$

Construct	Cultures showing action potential-induced Ca^{2+} transients*		Responsive myotubes per dish‡	
	%	*n*		*n*
GFP-α_{1S}	95	22	26.6 ± 22.2	14
GFP-α_{1C}	100	22	27.9 ± 23.5	22
GFP-α_{1A}	22	23	0.2 ± 0.4	22
GFP-α_1Aas$_{(1592\text{-clip})}$	60	43	1.8 ± 2.4	40

*Percentages of culture dishes with one or more responsive myotubes of number of dishes (*n*) tested.
‡Standard deviation of the mean of *n* dishes tested.

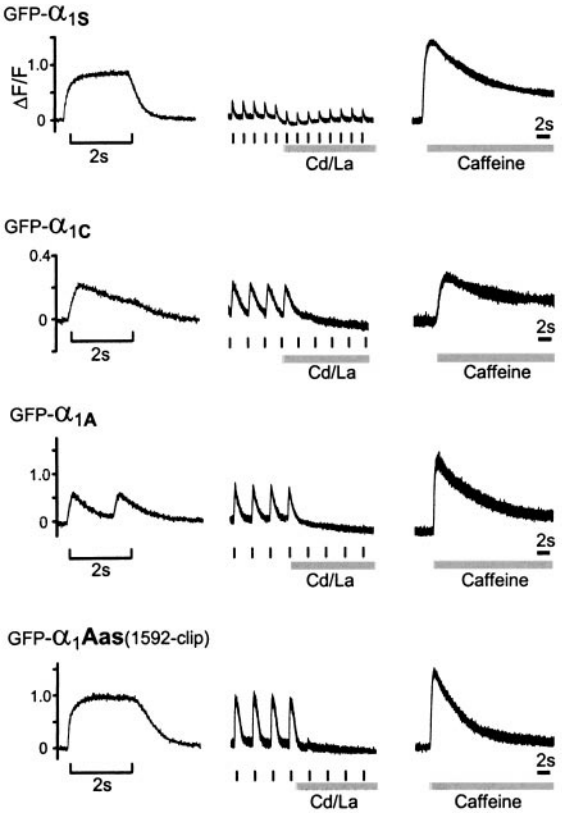

Figure 7. Restoration of EC coupling by targeted and nontargeted Ca^{2+} channel isoforms. Action potential–induced Ca^{2+} transients were recorded in transfected dysgenic myotubes loaded with the fluorescent Ca^{2+} indicator Fluo4-AM, using tetanic electrical stimulation (left, 20 Hz, 2 s, bracket) or low frequency stimulation (center, 0.3–0.5 Hz as marked). 0.5 mM Cd^{2+}/0.1 mM La^{3+} (gray bar) was applied to block the Ca^{2+} influx during the low-frequency stimulation protocol. Ca^{2+} release from the SR could be triggered by the application of 6 mM caffeine (gray bar) to the bath after current block. Myotubes transfected with the skeletal GFP-α_{1S} responded to electrical stimulation with Ca^{2+} transients independently of Ca^{2+} influx. The cardiac GFP-α_{1C} also reconstituted EC coupling in dysgenic myotubes; however, Ca^{2+} transients stopped when the Ca^{2+} influx was blocked. Cardiac-type Ca^{2+} transients in response to electrical stimulation were rarely observed in dysgenic myotubes transfected with GFP-α_{1A} (see Table I) and about nine times more often with the targeted GFP-α_1Aas$_{(1592\text{-clip})}$. Example traces for each construct were recorded from the same myotubes in sequential order.

and 1661 of the skeletal muscle α_{1S} is sufficient to confer triad targeting properties to the neuronal α_{1A} subunit.

Comparing this sequence of α_{1S} with the corresponding sequences of the cardiac α_{1C}, which is also targeted to triads (Grabner et al., 1998), and with that of the nontargeted α_{1A} reveals surprisingly few residues that are conserved between α_{1S} and α_{1C} but distinct from α_{1A} (Fig. 6 a). However, replacing individual of these residues with alanin did so far not result in a loss of targeting properties (data not shown). Either a targeting motif within this 55 amino acid stretch of α_{1S} is made up of more than those residues conserved between α_{1S} and α_{1C}, or the signal that is contained in this sequence stretch of α_{1S} is located outside the corresponding region of α_{1C} (see below). To distinguish between these possibilities, the corresponding targeting signal in α_{1C} and other α_1 isoforms needs to be localized and extensive single and combinatorial amino acid mapping needs to be performed.

The importance of COOH-terminal sequences in targeting and immobilization in specialized neuronal membrane domains has been demonstrated for ligand- and voltage-gated ion channels (Sheng and Pak, 1999; Lim et al., 2000). To our knowledge, the sequence between 1607 and 1661 of α_{1S} contains only one known consensus protein binding site. The sequence SPV in position 1640–1642 corresponds to the PDZ-binding motif S/TXV; however, it is not positioned at the very COOH terminus as is the case in the majority of reported PDZ-binding proteins (Sheng, 1996). Using a yeast–two-hybrid assay, Proenza et al. (2000) recently observed that this motif is part of a highly reactive region in the COOH terminus of α_{1S} and that substitution of the valine within this motif by aspartate abolished the high reactivity. This makes the PDZ-binding motif within the region demonstrated to contain the triad targeting signal in the present study a good candidate for protein–protein interactions that may contribute to triad targeting. However, the corresponding sequence in α_{1C} lacks the critical valine of this motif. Thus, if binding to PDZ proteins were the mechanism of triad targeting, other PDZ-binding motifs located elsewhere in the channel had to be responsible for the same function in the cardiac isoform. Two such motifs exist in the COOH terminus of α_{1C}, however, immediately distally to the putative clipping site. Other evidence for the importance of the COOH terminus in membrane targeting comes from heterologous expression of the cardiac α_{1C} in tsA201 cells (Gao et al., 2000). However, the region identified in that study to be important for functional membrane expression of α_{1C} is in the proximal, highly homologous part of the COOH terminus, ending 69 amino acids upstream of the region corresponding to the triad targeting signal identified in our study using a gain-of-function approach. Assuming that the loss of function in response to COOH-terminal truncations and deletions arose from specific effects on the targeting process rather than from nonspecific damage to the expressed channel, this domain is most likely not involved in the highly specific insertion of the channel into triad junctions, but may be important for a more general aspect like the export from the ER or membrane incorporation. Our present results do not exclude the possible contribution of other signals, shared by α_{1S} and α_{1A}, to the complex process that culminates in triad targeting.

Effects of Triad Targeting of GFP-α_1Aas$_{(1592\text{-clip})}$ on Ca^{2+} Currents and EC Coupling

Comparison of the current properties of GFP-α_{1A} and GFP-α_1Aas$_{(1524\text{-}1591)}$, both of which are not targeted into the triad, with that of the targeted GFP-α_1Aas$_{(1592\text{-clip})}$ provides additional evidence for the existence of distinct mechanisms for membrane and triad targeting (Fig. 6, b and c). Compared with GFP-α_{1A}, GFP-α_1Aas$_{(1524\text{-}1591)}$ exhibited strongly reduced current densities, even though the immunolabeling experiments gave no indication that the transfection efficiency or the amount of protein expressed had been decreased. It was necessary to increase the concentration of the charge carrier from 3 to 10 mM Ca^{2+} (Fig. 6 c) to show that this chimera did in fact express functional channels in the membrane; however, at strongly reduced levels. This suggested that in this chimera a distinct

signal important for membrane expression of α_{1A} had been abolished, but that this loss had not been compensated by the addition of the skeletal muscle triad targeting signal. To find out whether this putative membrane insertion signal of α_{1A} resides in the region replaced by the skeletal sequence (1524–1591) or whether it is contained in the distal portion of the COOH terminus that had been truncated in this chimera, we generated a truncated GFP-α_{1A} and expressed it in the dysgenic myotubes (data not shown). Current expression of this GFP-$\alpha_{1A\text{-clip}}$ was also low, suggesting that the distal COOH terminus of α_{1A} contains a separate signal that is important for its efficient membrane expression, but is not sufficient for triad targeting.

Considering the fact that our final triad-targeting chimeras lack this α_{1A} membrane-targeting signal, it is even more astonishing that the skeletal residues 1592–1661 not only fully compensated the loss of current expression caused by the truncation of α_{1A}, but that current densities of the targeted GFP-α_1Aas$_{(1592\text{-clip})}$ were increased by approximately twofold over those of the wild-type α_{1A} (Fig. 6 c). Among several possible causes for this effect, an increase in current density accompanying triad targeting is consistent with a model by which the specific incorporation into the triadic complex stabilizes the channel in the membrane, thus leading to an increased total number of functional channels.

Finally, to the question of how the localization of a Ca^{2+} channel in skeletal muscle affects EC coupling. The two muscle isoforms, α_{1S} and α_{1C}, which are both targeted into triads, have repeatedly been shown to rescue EC coupling in dysgenic myotubes (Tanabe et al., 1988 and 1990b; Grabner et al., 1998; Neuhuber et al., 1998b; Flucher et al., 2000). However, the mechanism by which the skeletal muscle α_{1S} and the cardiac α_{1C} activate SR Ca^{2+} release in dysgenic myotubes differs. In α_{1S}, it functions independently of Ca^{2+} influx, whereas α_{1C} does require Ca^{2+} influx for the activation of EC coupling. In Fig. 7, we show that dysgenic myotubes transfected with GFP-α_{1S} or GFP-α_{1C} respond to electrical stimulation with strong Ca^{2+} transients, which have previously been described as action potential–induced Ca^{2+} transients based on their all-or-none characteristics (Flucher et al., 1994; Powell et al., 1996). With GFP-α_{1S}, these Ca^{2+} transients continued after blocking the Ca^{2+} currents by the addition of Cd^{2+}/La^{3+} to the bath solution, whereas with GFP-α_{1C} the Ca^{2+} transients ceased, confirming that this SR Ca^{2+} release was Ca^{2+}-induced. Caffeine induced strong Ca^{2+} transients even after the Cd^{2+}/La^{3+} block, indicating that the cessation of Ca^{2+} transients was not due to depletion of the SR Ca^{2+} stores or damage to the release mechanism.

Previous attempts to rescue EC coupling in dysgenic myotubes by expressing the neuronal α_{1A} failed to display (Grabner et al., 1998), or only very rarely displayed, evoked contractions (Adams et al., 1994), despite the fact that α_{1A} expressed sizable Ca^{2+} currents. Using a more direct method to monitor SR Ca^{2+} release with the fluorescent Ca^{2+} indicator fluo-4, we did observe rare action potential–induced Ca^{2+} transients in GFP-α_{1A}–transfected myotubes (Table I and Fig. 7). While >25 responsive myotubes were found in almost all of GFP-α_{1S}– and GFP-α_{1C}–transfected cultures, on average only every fifth culture transfected with GFP-α_{1A} contained one or two responsive myotubes. The degree of restoration of EC coupling increased significantly ($P = 0.002$) when the class-A channel was targeted into the triad. In myotubes transfected with GFP-α_1Aas$_{(1592\text{-clip})}$, action potential–induced Ca^{2+} transients were observed in 60% of the cultures (Table I). As expected, these Ca^{2+} transients could be blocked with Cd^{2+}/La^{3+}, indicating that the mechanism by which GFP-α_1Aas$_{(1592\text{-clip})}$ restored EC coupling was Ca^{2+}-induced Ca^{2+} release (Fig. 7).

The enhanced restoration of EC coupling by the targeting of a class-A channel into the triads shows the importance of the correct localization of the Ca^{2+} channel in close proximity to the SR Ca^{2+} release channel. Apparently, the large Ca^{2+} influx through α_{1A} distributed throughout the plasma membrane was not sufficient to induce Ca^{2+}-induced Ca^{2+} release except in a few myotubes. However, concentrating the Ca^{2+} current to the restricted spaces of the triadic compartments strongly improved the chance of reaching the threshold for Ca^{2+}-induced Ca^{2+} release. This interpretation is consistent with other cellular processes where the close proximity of a Ca^{2+} source and a Ca^{2+} target is required for normal function (e.g., the association of the RyR and the Ca^{2+}-activated potassium channel in smooth muscle cells; Jaggar et al., 2000) and highlights the importance of specific targeting mechanisms for Ca^{2+} channels.

The more we learn about Ca^{2+} channels in their native environments, the more it appears to be the rule rather than the exception that they are specifically localized in functional domains. The signal contained in the 55 amino acid sequence of the COOH terminus of α_{1S} is the first description of a targeting signal of a voltage-gated Ca^{2+} channel for a specific membrane domain. It may share its anchoring mechanism with other ion channels that have been shown to interact with proteins containing PDZ domains, but for which the importance of this protein–protein interaction in the targeting process has yet to be shown. The complex passage of the skeletal muscle Ca^{2+} channel from the biosynthetic apparatus into the triad junction involves multiple steps. At the beginning of the journey, the interaction of the β subunit with the I-II loop and with the COOH terminus seems to play an important role in the export of the channel from the ER and for its functional expression in the plasma membrane. At the end of the journey, the specific interaction with the RyR determines the tetradic organization of the α_{1S} subunit that structurally sets it apart from the cardiac α_{1C}. But between these two events occurs the essential targeting of the Ca^{2+} channel into the junctional domain of the triad, and the signal contained within residues 1607–1661 of the skeletal muscle α_{1S} subunit is necessary and sufficient to confer this targeting property to a neuronal α_1 subunit.

We thank Dr. J. Hoflacher and E. Emberger for their excellent experimental help, and Dr. H. Glossmann for generously providing support for the pursuit of this project.

This work was supported in part by the Fonds zur Förderung der wissenschaftlichen Forschung, Austria, grants P12653-MED (B.E. Flucher), and P13831-GEN (M. Grabner), and by the European Commission's Training and Mobility of Researchers Network grant ERBFMRXCT960032 (B.E. Flucher).

Submitted: 1 August 2000
Revised: 6 September 2000
Accepted: 7 September 2000

References

Adams, B.A., T. Tanabe, A. Mikami, S. Numa, and K.G. Beam. 1990. Intramembrane charge movement restored in dysgenic skeletal muscle by injection of dihydropyridine receptor cDNAs. *Nature.* 346:569–572.

Adams, B.A., Y. Mori, M.S. Kim, T. Tanabe, and K.G. Beam. 1994. Heterologous expression of BI Ca^{2+} channels in dysgenic skeletal muscle. *J. Gen. Physiol*. 104:985–996.

Beam, K.G., B.A. Adams, T. Niidome, S. Numa, and T. Tanabe. 1992. Function of a truncated dihydropyridine receptor as both voltage sensor and calcium channel. *Nature*. 360:169–171.

Berridge, M.J. 1998. Neuronal calcium signaling. *Neuron.* 21:13–26.

Beurg, M., M. Sukhareva, C. Strube, P.A. Powers, R.G. Gregg, and R. Coronado. 1997. Recovery of Ca^{2+} current, charge movements, and Ca^{2+} transients in myotubes deficient in dihydropyridine receptor β_1 subunit transfected with β_1 cDNA. *Biophys. J.* 73:807–818.

Bichet, D., V. Cornet, S. Geib, E. Carlier, S. Volsen, T. Hoshi, Y. Mori, and M. De Waard. 2000. The I-II loop of the Ca^{2+} channel α_1 subunit contains an endoplasmic reticulum retention signal antagonized by the β subunit. *Neuron.* 25:177–190.

Block, B.A., T. Imagawa, K.P. Campbell, and C. Franzini-Armstrong. 1988. Structural evidence for direct interaction between the molecular components of the transverse tubule/sarcoplasmic reticulum junction in skeletal muscle. *J. Cell Biol.* 107:2587–2600.

Brice, N.L., N. S. Berrow, V. Campbell, K.M. Page, K. Brickley, I. Tedder, and A.C. Dolphin. 1997. Importance of the different β subunits in the membrane expression of the α_{1A} and α_2 calcium channel subunits: studies using a depolarization-sensitive α_{1A} antibody. *Eur. J. Neurosci.* 9:749–759.

Catterall, W.A. 1996. Molecular properties of sodium and calcium channels. *J. Bioenerg. Biomembr.* 28:219–230.

Chien, A.J., X. Zhao, R.E. Shirokov, T.S. Puri, C.F. Chang, D. Sun, E. Ríos, and M.M. Hosey. 1995. Roles of a membrane-localized β subunit in the formation and targeting of functional L-type Ca^{2+} channels. *J. Biol. Chem*. 270: 30036–30044.

De Jongh, K.S., C. Warner, A.A. Colvin, and W.A. Catterall. 1991. Characterization of the two size forms of the α1 subunit of skeletal muscle L-type calcium channels. *Proc. Natl. Acad. Sci. USA*. 88:10778–10782.

Flucher, B.E., M.E. Morton, S.C. Froehner, and M.P. Daniels. 1990. Localization of the α_1 and α_2 subunits of the dihydropyridine receptor and ankyrin in skeletal muscle triads. *Neuron.* 5:339–351.

Flucher, B.E., J.L. Phillips, and J.A. Powell. 1991. Dihydropyridine receptor α subunits in normal and dysgenic muscle in vitro: expression of α_1 is required for proper targeting and distribution of α_2. *J. Cell Biol.* 115:1345–1356.

Flucher, B.E., S.B. Andrews, and M.P. Daniels. 1994. Molecular organization of transverse tubule/sarcoplasmic reticulum junctions during development of excitation–contraction coupling in skeletal muscle. *Mol. Biol. Cell*. 5:1105–1118.

Flucher, B.E., N. Kasielke, U. Gerster, B. Neuhuber, and M. Grabner. 2000. Insertion of the full-length calcium channel α_{1S} subunit into triads of skeletal muscle in vitro. *FEBS Lett*. 474:93–98.

Franzini-Armstrong, C., and A.O. Jorgensen. 1994. Structure and development of E-C coupling units in skeletal muscle. *Annu. Rev. Physiol*. 56:509–534.

Freise, D., B. Held, U. Wissenbach, A. Pfeifer, C. Trost, N. Himmerkus, U. Schweig, M. Freichel, M. Biel, F. Hofmann, et al. 2000. Absence of the γ subunit of the skeletal muscle dihydropyridine receptor increases L-type Ca^{2+} currents and alters channel inactivation properties. *J. Biol. Chem.* 275: 14476–14481.

Gao, T., M. Buenemann, B.L. Gerhardstein, H. Ma, and M.M. Hosey. 2000. Role of the C-terminus of the α_{1C} (CaV1.2) subunit in membrane targeting of cardiac L-type calcium channels. *J. Biol Chem.* 275:25436–25444

Giannini, G., A. Conti, S. Mammarella, M. Scrobogna, and V. Sorrentino. 1995. The ryanodine receptor/calcium channel genes are widely and differentially expressed in murine brain and peripheral tissues. *J. Cell Biol.* 128:893–904.

Grabner, M., A. Bachmann, F. Rosenthal, J. Striessnig, C. Schulz, D. Tautz, and H. Glossmann. 1994. Insect calcium channels: molecular cloning of an α_1 subunit from housefly (*Musca domestica*) muscle. *FEBS Lett.* 339:189–194.

Grabner, M., R.T. Dirksen, and K.G. Beam. 1998. Tagging with green fluorescent protein reveals a distinct subcellular distribution of L-type and non–L-type Ca^{2+} channels expressed in dysgenic myotubes. *Proc. Natl. Acad. Sci. USA*. 95:1903–1908.

Grabner, M., R.T. Dirksen, N. Suda, and K.G. Beam. 1999. The II-III loop of the skeletal muscle dihydropyridine receptor is responsible for the bi-directional coupling with the ryanodine receptor. *J. Biol. Chem.* 274:21913–21919.

Gregg, R.G., A. Messing, C. Strube, M. Beurg, R. Moss, M. Behan, M. Sukhareva, S. Haynes, J.A. Powell, R. Coronado, and P.A. Powers. 1996. Absence of the β subunit (cchβ1) of the skeletal muscle dihydropyridine receptor alters expression of the α_1 subunit and eliminates excitation–contraction coupling. *Proc. Natl. Acad. Sci. USA*. 93:13961–13966.

Horton, R.M., H.D. Hunt, S.N. Ho, J.K. Pullen, and L.R. Pease. 1989. Engineering hybrid genes without the use of restriction enzymes: gene splicing by overlap extension. *Gene.* 77:61–68.

Jaggar, J.H., VA.Porter, W.J. Lederer, and M.T. Nelson. 2000. Calcium sparks in smooth muscle. *Am. J. Physiol. Cell Physiol*. 278:C235–C256.

Jorgensen, A.O., A.C.-Y. Shen, W. Arnold, A.T. Leung, and K.P. Campbell. 1989. Subcellular distribution of the 1,4-dihydropyridine receptor in rabbit skeletal muscle in situ: an immunofluorescence and immunocolloidal gold-labeling study. *J. Cell Biol.* 109:135–147.

Lim, S.T., D.E. Antonucci, R.H. Scannevin, and J.S. Trimmer. 2000. A novel targeting signal for proximal clustering of the Kv2.1 K^+ channel in hippocampal neurons. *Neuron*. 25:385–397.

Melzer, W., A. Herrmann-Frank, and H.C. Luttgau. 1995. The role of Ca^{2+} ions in excitation–contraction coupling of skeletal muscle fibres. *Biochim. Biophys. Acta*. 1241:59–116.

Mori, Y., T. Friedrich, M.-S. Kim, A. Mikami, J. Nakai, P. Ruth, E. Bosse, F. Hofmann, V. Flockerzi, T. Furuichi, et al. 1991. Primary structure and functional expression from complementary DNA of a brain calcium channel. *Nature.* 350:398–402.

Morton, M.E., and S.C. Froehner. 1987. Monoclonal antibody identifies a 200-kDa subunit of the dihydropyridine-sensitive calcium channel. *J. Biol. Chem*. 262:11904–11907.

Nakai, J., R.T. Dirksen, H.T. Nguyen, I.N. Pessah, K.G Beam, and P.D. Allen. 1996. Enhanced dihydropyridine receptor channel activity in the presence of ryanodine receptor. *Nature.* 380:72–75.

Neuhuber, B., U. Gerster, J. Mitterdorfer, H. Glossmann, and B.E. Flucher. 1998a. Differential effects of Ca^{2+} channel β_{1a} and β_{2a} subunits on complex formation with α_{1S} and on current expression in tsA201 cells. *J. Biol. Chem.* 273:9110–9118.

Neuhuber, B., U. Gerster, F. Doring, H. Glossmann, T. Tanabe, and B.E. Flucher. 1998b. Association of calcium channel α_{1S} and β_{1a} subunits is required for the targeting of β_{1a} but not of α_{1S} into skeletal muscle triads. *Proc. Natl. Acad. Sci. USA*. 95:5015–5020.

Powell, J.A., L. Petherbridge, and B.E. Flucher. 1996. Formation of triads without the dihydropyridine receptor α subunits in cell lines from dysgenic skeletal muscle. *J. Cell Biol.* 134:375–387.

Pragnell, M., M. De Waard, Y. Mori, T. Tanabe, T.P. Snutch, and K.P. Campbell. 1994. Calcium channel β-subunit binds to a conserved motif in the I-II cytoplasmic linker of the α_1-subunit. *Nature.* 368:67–70.

Proenza, C., C. Wilkens, N.M. Lorenzon, and K.G. Beam. 2000. A carboxyl-terminal region important for the expression and targeting of the skeletal muscle dihydropyridine receptor. *J. Biol. Chem.* 275:23169–23174.

Protasi, F., C. Franzini-Armstrong, and P.D. Allen. 1998. Role of ryanodine receptors in the assembly of calcium release units in skeletal muscle. *J. Cell Biol*. 140:831–842.

Ríos, E., G. Pizarro, and E. Stefani. 1992. Charge movement and the nature of signal transduction in skeletal muscle excitation–contraction coupling. *Annu. Rev. Physiol*. 54:109–133.

Sheng, M. 1996. PDZs and receptor/channel clustering: rounding up the latest suspects. *Cell.* 17:575–578.

Sheng, M., and D.T. Pak. 1999. Glutamate receptor anchoring proteins and the molecular organization of excitatory synapses. *Ann. NY Acad. Sci.* 868:483–493.

Takekura, H., M. Nishi, T. Noda, H. Takeshima, and C. Franzini-Armstrong. 1995. Abnormal junctions between surface membrane and sarcoplasmic reticulum in skeletal muscle with a mutation targeted to the ryanodine receptor. *Proc. Natl. Acad. Sci. USA*. 92:3381–3385.

Tanabe, T., H. Takeshima, A. Mikami, V. Flockerzi, H. Takahashi, K. Kangawa, M. Kojima, H. Matsuo, T. Hirose, and S. Numa. 1987. Primary structure of the receptor for calcium channel blocker from skeletal muscle. *Nature.* 328:313–318.

Tanabe, T., K.G. Beam, J.A. Powell, and S. Numa. 1988. Restoration of excitation–contraction coupling and slow Ca^{2+} current in dysgenic muscle by dihydropyridine receptor complementary DNA. *Nature.* 336:134–139.

Tanabe, T., K.G. Beam, B.A. Adams, T. Niidome, and S. Numa. 1990a. Regions of the skeletal muscle dihydropyridine receptor critical for excitation–contraction coupling. *Nature*. 346:567–569.

Tanabe, T., A. Mikami, S. Numa, and K.G. Beam. 1990b. Cardiac-type excitation–contraction coupling in dysgenic skeletal muscle injected with cardiac dihydropyridine receptor cDNA. *Nature.* 344:451–453.

Walker, D., D. Bichet, K.P. Campbell, and M. De Waard. 1998. A β_4 isoform-specific interaction site in the carboxyl-terminal region of the voltage-dependent Ca^{2+} channel α_{1A} subunit. *J. Biol. Chem*. 173:1361–1367.